Advances in Science and Technology Research Journal

Advances in Science and Technology Research Journal 2024, 18(3), 140–150
https://doi.org/10.12913/22998624/186159
ISSN 2299-8624, License CC-BY 4.0

Received: 2024.03.08
Accepted: 2024.03.22
Published: 2024.04.20

Surface Modification of the Ti-35Nb-7Zr-5Ta Bio Alloy by the PM-EDM Route

Ahmed Rabeea Hayyawi[1*], Haydar Al-Ethari[1], Ali Hubi Haleem[1]

[1] Department of Metallurgical Eng., Materials Eng. College, University of Babylon, Iraq

* Corresponding author's e-mail: ahmed.hayyawi.math45@student.uobabylon.edu.iq

ABSTRACT

One of the most attractive β-Ti alloys is Ti–35Nb–7Zr–5Ta wt% (TNZT) alloy, which has one of the lowest Young's moduli among the β-Ti family (about 55 GPa) and contains no cytotoxic elements. On the other hand, the β-type Ti alloys are susceptible to bacterial infection because they lack an antibacterial function and can become contaminated quickly after implantation, making surface modification a keyway to improve the antibacterial properties of these alloys. A recently created technique called powder mixed-EDM can simultaneously improve machining, mechanical, and biological properties. In this research, silver was added to the dielectric fluid during PM-EDM of Ti-35Nb-7Zr-5Ta wt% alloy prepared by powder metallurgy route. The surface composition, Brinell hardness, corrosion resistance, ion release, and antibacterial properties were evaluated for the TNZT alloy before and after surface modification. The results show better hardness and corrosion resistance as well as lower ion release for the PM-EDMed specimen due to the presence of Ag, oxides, and carbides such as NbC, TiC, TiO_2, ZrO_2, and Nb_2O_5 that is deposited and embedded as a hard phase in the recast layer of the machined surface. Also, the antibacterial property of the PM-EDMed specimen is effectively improved as silver is an antibiotic with a wide range, so it has favorable antibacterial properties for Gram-negative and Gram-positive bacteria.

Keywords: TNZT alloy, biocompatibility, surface modification, PM-EDM, silver, antibacterial property.

INTRODUCTION

Of all the available metallic biomaterials, Ti and Ti-alloys have the best biocompatibility in terms of osteogenesis. Ti alloys are also thought to be good substitutes for the commercially available Co-Cr and stainless-steel alloys, which are employed as biomaterials in implant devices. Because the β Ti-alloys usually have a lower elastic modulus than the α- or (α + β) Ti-alloys, researchers have concentrated their efforts on producing the β Ti-alloys with the lowest feasible elastic modulus [1]. Ti-35Nb-7Zr-5Ta (TNZT), Ti-29Nb-13Ta-4.6Zr (TNTZ), and Ti-36Nb-2Ta-3Zr-O (gum metal) are the low modulus β-Ti alloys with the most biocompatible elements; their respective elastic modulus values are about (55, 60, and 70) GPa. Since Nb, Ta, and Zr have been shown to be safe for humans, it would be ideal to find a way to reduce the elastic modulus of the β-Ti alloy system [2]. The Ti–35Nb–7Zr–5Ta wt% alloy is one of the most attractive β-Ti alloys [3], it has no cytotoxic components and one of the lowest moduli of elasticity (about 55 GPa) in the β-Ti family. Studies showed that this alloy has a low Young's modulus and sufficiently high plasticity, no cytotoxicity, and the lowest risks of allergy responses. It also has great corrosion resistance, biocompatibility, and excellent chemical stability in corrosive conditions [4].

The term "antibacterial property" refers to a capacity of the material to maintain its effectiveness in the presence of bacteria or other microbes, and it is one of the primary requirements for biomaterials [5]. Because they lack an antibacterial function and can become contaminated quickly after implantation, β-type Ti alloys are

susceptible to bacterial infection, making surface modification a keyway to improve the antibacterial properties of these alloys [6]. Surface modification is regarded by academics, engineers, and medical surgeons as a critical approach for mitigating possible biological and physical reactions to implants. Furthermore, the surface coating has better bioactivity and host responses, better bone formability, and increased resistance to wear and corrosion [7]. A recently created technique called powder mixed-EDM is included in the EDM to enhance its performance, primarily with the die-sink EDM. Metal powders are added to the EDM oil depending on the intended use, which enhances the surface properties and operational performance of workpiece. The conductive particles combined with the dielectric liquid diminish the breakdown strength of the insulator fluid by widening the discharge channel, which lowers the electrical intensity across the machining spot and leaves tiny craters behind [8]. Furthermore, the bridging effect of the added powders facilitates the dispersion of electrical sparks, giving the surface the appropriate roughness. There is an almost 100% increase in the void between the electrode and the tool to be machined, going from (25–50) to (50–150) μm [9]. Many powders are used for PM-EDM. Generally, the favorable powder characteristics are high electrical and thermal conductivity, low density, and biocompatibility in the machining of implants. High thermal conductivity means more heat is distributed and dissipated to the surface of the workpiece to limit the size of craters produced. Low electrical resistivity creates a high spark and high thermal conductivity takes more heat away. Usually, the gap width is significantly influenced by the conductivity of the powder. Conductive powders always yield a larger gap width than semi-conductive powders [10]. Additionally, the dispersion of sparks from the more electrically conductive particles may result in fewer microcracks and residual stresses on the surface [11]. Prior to the discovery of penicillium, silver (Ag), an antibacterial metal, was used in medicine. Numerous studies on the use of Ag to modify bioimplant surfaces demonstrate how this improves cytocompatibility [12]. The temperature range between 8000 °C and 15000 °C is created by electrical sparks. Consequently, the powders melt, and the materials fall off from the electrode and work material surfaces [13]. The molten powders stick to the electrode surface readily because of electromagnetic forces and the negative pressure of electrophoresis, since the powder particles store ions and electrons on their surfaces and the gap distance is extremely small. The decomposition of the dielectric liquid produces a simultaneous supply of carbon, hydrogen, and oxygen. Because of the high-temperature production caused by the reaction of ions with one another, the compounds are created that melt simultaneously. In addition, a quick temperature decrease in the gap causes the molten metals to solidify because the dielectric fluid serves as a flushing system, coolant, and insulation. The workpiece surface is carefully formed during this process, and alloying oxides, bioactive compounds, and carbides further modify the workpiece's composition and topography [14]. Researchers are very interested in the novel use of PM-EDM called surface treatment since it allows for simultaneous surface modification and implant shaping. Katsushi Furutania et al. [15], investigated the creation of a thick TiC or WC layer using EDM and a green compact electrode. The green compact electrode provides tungsten or titanium alloy powder, which is attracted to a workpiece by the heat of the discharge. It is possible to maintain a high concentration of Ti powder in the gap between a workpiece and a rotating disk electrode by suspending it in working oil, such as kerosene. On carbon steel with a 1 mm diameter electrode, a 150 μm thick TiC layer with a hardness of 1600 HV forms. Prakash et al. [16], modified the β-Ti implant by adding silicon powder to the dielectric fluid during the PM-EDM process in order to enhance its surface properties. The usage of PM-EDM changed the surface topography and provided surface chemistry with oxides and carbides. Due to the hard carbide phases forming on the machined layer, the microhardness of the PM-EDMed surface has risen twice compared to the base material. The tribological investigation has demonstrated that the modified layer exhibits superior wear resistance and great friction reduction compared to the unmachined samples. The development of carbides resembling TiC, NbC, and SiC on the machined surface has been credited with these results. Prakash et al. [17], investigated hydroxyapatite-mixed EDM of the Ti-35Nb-7Zr-5Ta implant to improve its in-vitro bioactivity and corrosion resistance. The findings of the morphology characterization showed that the implant surface has been given a naturally occurring nano-porous surface topography that matches bone. The deposited layer, which formed biocompatible

phases like $Ca_3(PO_4)_2$, $CaZrO_3$, Nb_8P_5, CaO, TiP, Nb_4O_5, and TiO_2, TiH on the implant surface, was composed of titanium, niobium, tantalum, zirconium, oxygen, calcium, and phosphorous elements, according to the EDS and XRD analyses. This enhanced the alloy bioactivity and was advantageous for the promotion of osseointegration. Davis et al. [18], investigated PM-EDM surface modification of biomedical Ti-6Al-4V alloy. This study modified the current capabilities of a conventional EDM system by varying the concentration of bioactive zinc powder particles in the dielectric by 0, 2, 4, 6, 8, and 10 g/l. The analytical results show that PM-EDM has lower dimensional deviation, recast layer thickness, and machining time than conventional EDM. An extensive analysis of this surface confirmed a notable alteration in terms of better wettability (contact angle < 90°), topography (Ra = 743.65 nm), and recast layer thickness (26.44 μm), indicating its potential use in dentistry. Further encouraging in vitro cytocompatibility as well as ZnO and TiO observations in X-ray diffraction are later biological and therapeutic tests that confirm the predicted antiviral efficacy of the modified Ti-6Al-4V alloy surface against coronavirus (COVID-19). Schubert et al. [19], studied the surface modification of Ti-6Al-4V surface using nano silver powder in dielectric fluid by PM-EDM operation. The distribution of powder particles in the machining gap is largely dependent on the dielectric flow, and this has a large impact on the powder deposition onto the modified surface. The findings indicate that PM-EDM is a promising approach for combined antibacterial surface modification and machining of medical implants. Nurlan et al. [20], investigated the impact of hydroxyapatite (HA) powder-mixed EDM (PM-EDM) on the antibacterial characteristics of Ti-6Al-4V alloy. The Pseudomonas aeruginosa, Bacillus subtilis, Escherichia coli, and Staphylococcus aureus microorganisms were tested for antibacterial activity. The main findings demonstrated a relationship between the antibacterial qualities of modified surfaces and the discharge energy as well as powder concentration. The modified surfaces demonstrated decreased biofilm development at low discharge energy and a 0 g/L concentration of powder, culminating in roughness of 0.273 μm. At a 10 g/L powder concentration and high discharge energy, this pattern held true with a 1.832 μm roughness. As a result, by adjusting the surface roughness, the antibacterial qualities may be optimized. It can be concluded that there are few researchers investigating the surface modification of Ti-35Nb-7Zr-5Ta by PM-EDM technique for biomedical applications. The surface modification of this alloy by the PM-EDM method using hydroxyapatite powder only was investigated [17]. On the other hand, most surface modification research by PM-EDM studied Ti-6Al-4V alloy using different powders and parameters. Also, there are no researchers who added silver powder in the PM-EDM process for surface modification of Ti-35Nb-7Zr-5Ta alloy. Silver powder in PM-EDM for surface modification but for Ti-6Al-4V alloy was used [19]. Thus, surface modification was done in this research for the Ti-35Nb-7Zr-5Ta alloy prepared by powder metallurgy using silver powder mixed EDM with proper evaluation for biocompatibility before and after the modification.

EXPERIMENTAL PROCEDURES

Materials and methods

PM-EDM operation is done for the Ti-35Nb-7Zr-5Ta alloy prepared by powder metallurgy. In order to achieve the experiments, a small specially designed tank was used instead of the machine tank to prevent powder suspension in the original tank filter and to reduce the used powder quantity. The newly designed tank has a circulating pump with an arm to direct the powder-mixed dielectric fluid to the electrode-workpiece region. Also, an external stirrer is used to prevent powder accumulation in the bottom of the tank. Figure 1 shows the experimental setup for the PM-EDM operation. The tool electrode is a cylinder-shaped, commercially pure Ti (grad 2) rod with a diameter of 12 mm. Eight liters of the dielectric fluid were placed in the machining container, and the hydrocarbon oil type HEDMA111 was utilized as the dielectric fluid. In this study, additives of Ag powder were used in the dielectric fluid. The top and bottom surfaces of the specimens are ground to make a well-leveled surface finish. The experiments have been conducted on the Electric Discharge Machine model (CM 323C CHMER). The experiments are done under different machining conditions that are mentioned in Table 1. Note that the base specimen is symbolized as (TNZT), while the PM-EDMed specimen is symbolized as (M-TNZT).

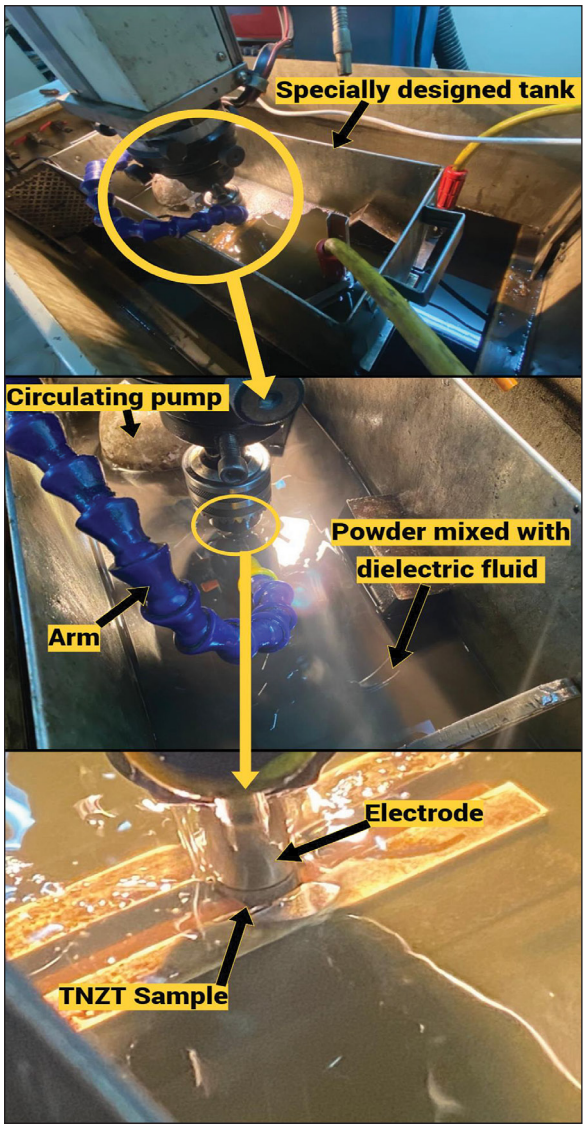

Figure 1. Experimental setup for PM-EDM operation used in this study

Surface morphology and chemistry analysis

Surface chemistry is very important for biomaterials to verify whether toxic substances are formed or not after PM-EDM operation. Therefore, surface chemistry was analyzed using the SEM-EDS device model (FEI, Quanta 450) in addition to the XRD device model (Labx XRD- 6000). Also, to ensure the concentration and distribution of added powder on the surface of the M-TNZT specimen, powder mapping is done using the same SEM-EDS device.

Brinell hardness test

According to ASTM (E10-15a) [21], the TNZT specimen was treated to the proper grinding and polishing process while the M-TNZT was taken as it was. A ball indenter with a diameter of 5 mm and a force of 306 N was used for 10 seconds using the Brinell hardness testing equipment model (HBRVS-187.5). Three hardness readings were averaged to determine the hardness.

Table 1. Machining parameters used in this study

Parameter	Description
Pulse current	5 A
Pulse on	9 µs
Pulse off	37 µs
Powder type	Ag
Powder concentration	20 g/L
Dielectric fluid	HEDMA111 hydrocarbon
Electrode	CP-grade II Ti
Polarity	Tool (+), workpiece (-)
Duty cycle	8%

Potentiodynamic polarization test

Electrochemical testing represents one of the corrosion measuring methods used to track the corrosion processes on a sample of the desired metal and examine the anodic and cathodic behaviors. A device type (winking M lab 200, Germany) was used for polarization experiments. The counter electrode was the Pt electrode, and the reference electrode was the SCE and working electrode (specimen) according to the ASTM (G5-14) [22]. Stepping the potential was done utilizing a 0.2 mV/s scanning rate from the initial potential of 250 mV below the OCP and continuing the scan up to 250 mV above the OCP. The corrosion resistance of the specimens was studied in SBF 37±1 °C. The following formula is used to determine the corrosion rate [23]:

$$CR = \frac{0.13\, I_{corr}(EW)}{\rho} \quad (1)$$

where: EW – equivalent weight (g/eq.), ρ – density (g/cm³), 0.13 – metric and time conversion factor, I_{corr} – corrosion current density (µA/cm²), and CR – corrosion rate (mils per year, mpy).

Metal ion release

To examine the safety and biocompatibility of the implants, it is important to understand how metal ions are released from metallic materials in vivo. The static immersion test was

carried out in accordance with the current JIS T- 0304 [24] metallic biomaterial requirements. An Atomic Absorption spectrophotometer type (VSI-2102) was used to calculate the ions release. Each specimen was immersed in plastic containers containing (50 ml) corrosive solutions (SBF) at 37 ± 1 °C for three weeks. The specimens were placed in a glass chamber to maintain a constant temperature of 37 ± 1 °C.

Antibacterial test

The surface of biomaterial was exposed to the risk of initial microbial colonization and bacterial attack. An antibacterial kinetic test is done using bacterial strains of *Staphylococcus aureus* (*S. aureus*, Gr^+) and *Escherichia coli* (*E. coli*, Gr^-). The inhibition zone approach was used to investigate the antibacterial activity. The circular region surrounding the antibiotic site where the bacterial colonies are not allowed to develop is known as the zone of inhibition. The bacteria's sensitivity to the antibiotic can be gauged using the zone of inhibition [25]. This test is done according to ISO 20645:2004 [26], using a Conrage stick, uniformly distributing the hot agar solution over the sterile Petri plates, and then allowing it to congeal in a sterile environment. For the bacteria preparation, a suspension of bacterium, *S. aureus* or *E. coli*, is sprayed equally overall the area of each Petri dish and placed in the incubator for 24 h at 37 °C. Then, the bacteria spread on a petri dish where the samples were placed on it and incubated. After that the inhibition zones were observed where the antibacterial capability is shown by the width of the inhibition zone, the greater the inhibition zone, the stronger the antibacterial activity.

RESULTS AND DISCUSSION

SEM/EDS and XRD analysis results

Figure 2 shows the EDS analysis of the PM-EDMed surface of the M-TNZT specimen. It can be clearly seen from this figure that the silver (Ag), oxygen (O), and carbon (C) exit on the M-TNZT surface with the base material of this alloy. The primary cause of the existence of C and O is the breakdown of hydrocarbon oil at high spark energy temperatures. As a result, the decomposed elements formed oxides and carbides such as TiC, TiO_2, and ZrO_2 on the machined surface, which may be expected to improve the surface quality. To ensure the presence of oxides and carbides on the PM-EDMed surface of the M-TNZT specimen, XRD was done and the results of the XRD analysis are shown in Figure 3.

Many oxides and carbides appeared in the XRD pattern, where TiO_2 appears in the angles 27.7°, 36.1°, 41.2°, 54.2° and 56.7°, according to the card (JCPDS Card No. 21-1272), ZrO_2 appears in the angles 30.15°, 50.15° and 60.11°, according to the card (JCPDS Card No. 79-1769), Nb_2O_5 appears in the angles 23.03° and 28.15° according

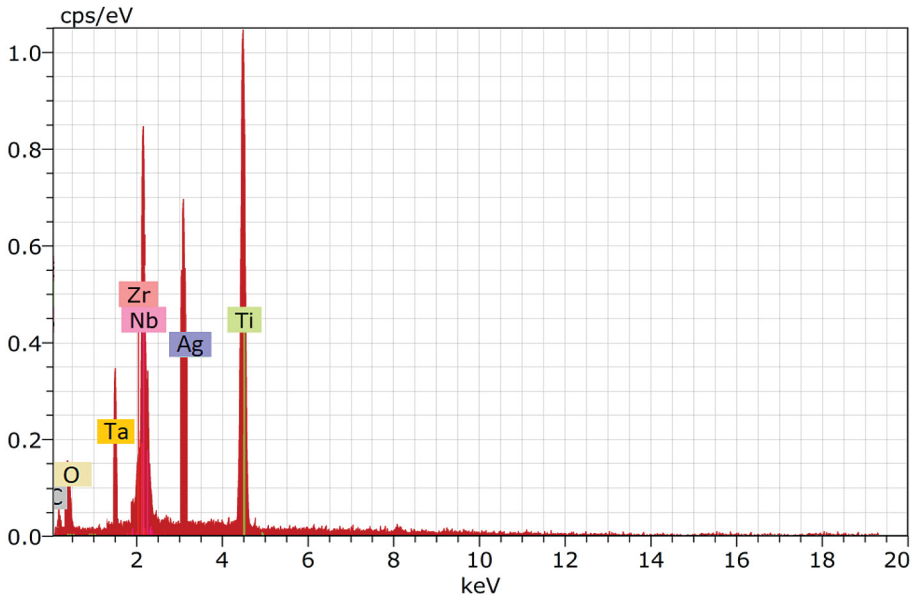

Figure 2. EDS analysis for M-TNZT surface

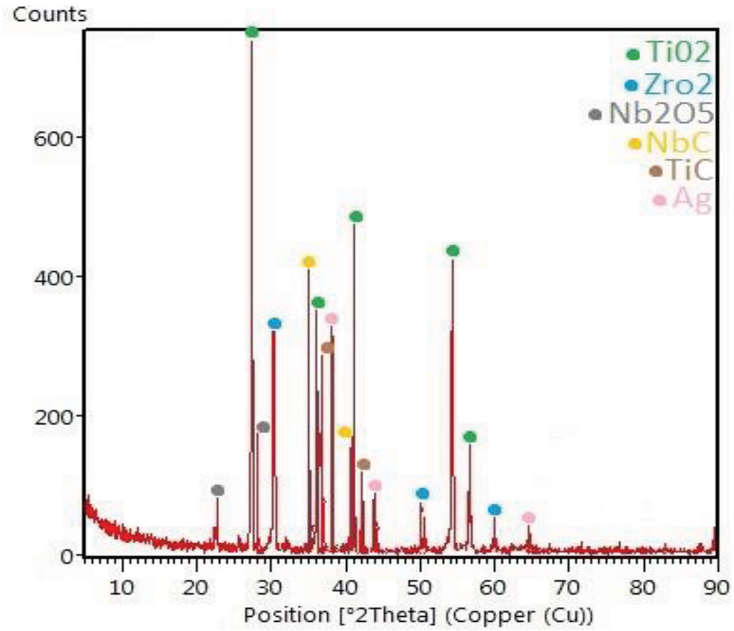

Figure 3. XRF chart for M-TNZT surface

to the card (JCPDS Card No. 30-0873), NbC appears in the angles 34.8° and 40.6° according to the card (JCPDS Card No. 38-1364), and TiC is appeared in the angles 36.9° and 42.0° according to the card (JCPDS Card No. 32-1383). It can be noticed that titanium oxide TiO_2 was the dominant oxide compared with the other oxides present in this chart. This is due to the fact that the affinity of oxygen to titanium is greater than its affinity to niobium or zirconium [27]. Tantalum oxide or carbide did not appear due to its low concentration in this alloy. On the other hand, silver has a low affinity to oxygen and carbon as it is a noble metal [28], so silver peaks appeared in the XRD chart rather than silver oxide or silver carbide as can be seen in the angles 38.1°, 44.17° and 64.53°, according to the card (JCPDS Card No. 04-0783). Implant surface coatings using these promising bio-ceramic oxides and carbides have been applied to improve the biocompatibility, hardness, and corrosion resistance of implants [29].

Silver mapping is done for the optimum machined alloy (M-TNZT) and the results are shown in Figure 4. Some silver was evidently adhered to the machined surface. The specimens were cleaned in an ultrasonic bath for ten minutes with their machined surfaces facing down, thus it is clear that the sticking phenomena were not brought on by silver powder settling during the cleaning procedure. According to the PM-EDM mechanism, some of the silver powder that was seen may have resulted from the spattering process, while the remaining portion may have

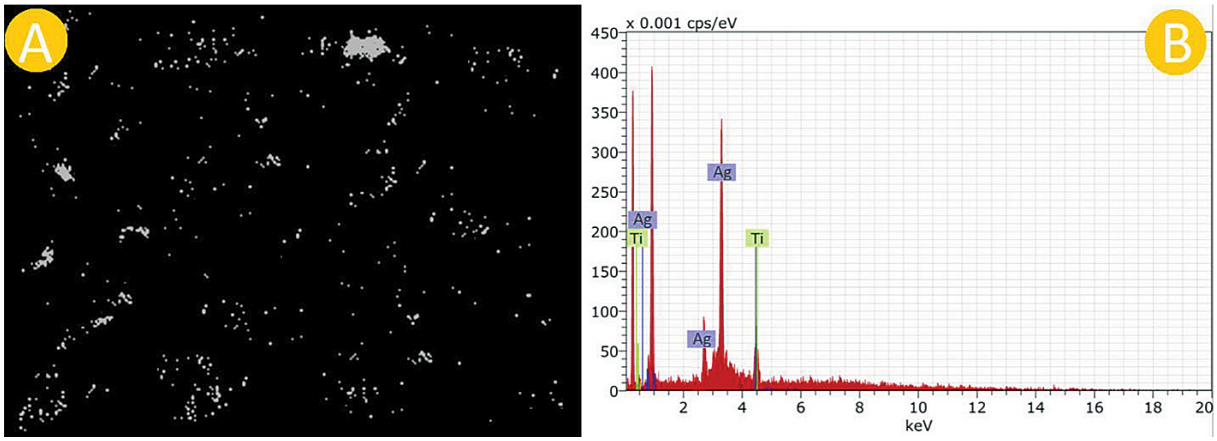

Figure 4. (a) Silver mapping for M-TNZT alloy, (b) EDS for the gray dots

come from a new dielectric fluid reflow. Silver is melted during machining and combined with other molten materials from the tool electrode and workpiece due to the extremely high temperature in the plasma channel (around 10,000 °C) and a thermal evaporation process. Following discharge, a process known as re-solidification creates the coating layer.

Brinell hardness analysis result

The Brinell hardness is 527 kg/mm^2 and 310 kg/mm^2 for the M-TNZT and TNZT specimens, respectively. HB value for the M-TNZT specimen is higher than that of the TNZT specimen by 70%. The increment in surface hardness in the M-TNZT specimen belongs to the heating and quenching operations that occurred to the machined surface. Also, the presence of Ag, oxides, and carbides such as NbC, TiC, TiO_2, ZrO_2, and Nb_2O_5 that have deposited and embedded as a hard phase in the recast layer of the machined surface, as shown in the XRD chart, increase the surface hardness of the M-TNZT alloy [30].

Potentiodynamic polarization test result

The Log current density-to-potential diagrams obtained from polarization in the SBF solution for TNZT and M-TNZT are shown in Figure 5. It can be noted that when the voltage is increased in cathodic polarization, the corrosion current drops until it attains its minimum value. When anodic polarization occurs, the corrosion current rises with voltage until it attains a point where the passive film forms and causes a sharp drop in voltage. At that point, the passive film breaks, and the current also rises [31]. Table 2 presents corrosion parameters obtained from the polarization curve for TNZT and M-TNZT alloys. From this table, it can be concluded that the corrosion rate for TNZT alloy is low due to the presence of beta stabilizer elements (Nb, Ta, and Zr) which increase the hardness and lead to the formation of a thicker oxide layer film, so passivity will increase and higher protection against corrosion will occur [32]. The current densities and potential for M-TNZT alloy, in this study, were lower in comparison with that of the TNZT alloy, thus corrosion resistance for the M-TNZT alloy is better. This can be attributed to the behavior of silver as an anti-corrosion and noble element, and the presence of oxides such as TiO_2, ZrO_2, and Nb_2O_5 (as was shown in the XRD pattern for the M-TNZT specimen) which in turn enhance the corrosion resistance of the M-TNZT alloy [33], where the current density is almost constant at the end of the polarization curve for M-TNZT specimen as a result to the passivation due to the formation of the overmentioned oxides and the ability to the reformation of these oxides (re-passivation) after the breakdown.

Ion release test result

Figures 6 and 7 show the amounts of metal ions released after immersion in SBF solution for 21 days at 37±1 °C for TNZT and M-TNZT alloys respectively.

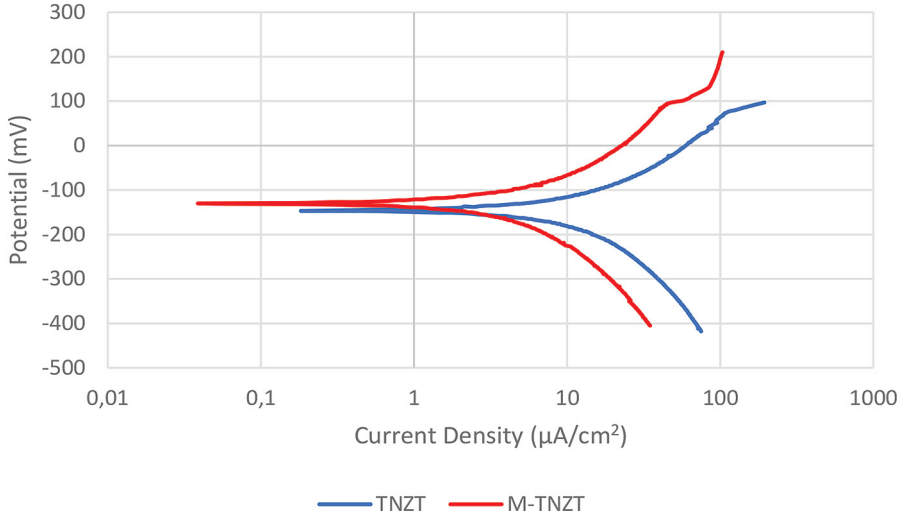

Figure 5. Potentiodynamic polarization for TNZT and M-TNZT specimens in SBF solution

Table 2. Corrosion parameters for TNZT and M-TNZT alloys in SBF solution

Alloy	E_{corr} (mV)	I_{corr} (μA/cm²)	Corrosion rate (mpy)	Improvement percentage (%)
TNZT	-144.3	4.02	0.011	/
M-TNZT	-131.0	0.493	0.001	91

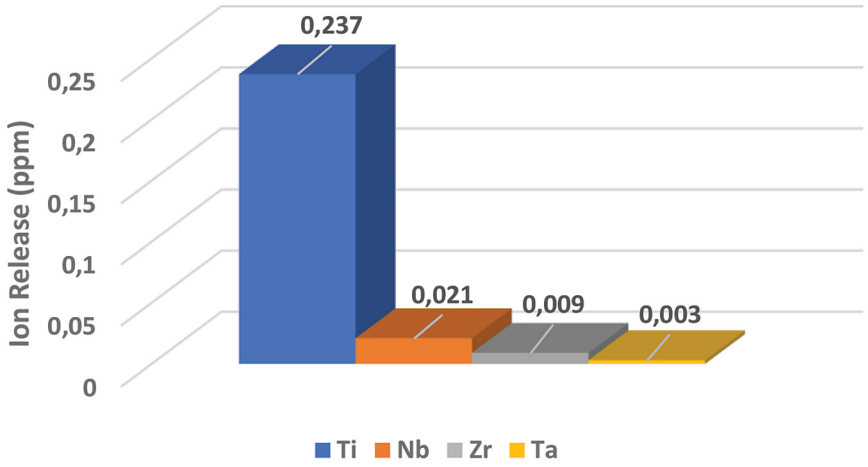

Figure 6. Quantity of metal ions released from TNZT alloy in SBF solution at 37 °C for 21 days

From Figure 6, it can be noticed that the metal ions released for the TNZT alloy in SBF solution have lower values due to the presence of beta stabilizing elements which stabilize and spread the beta phase in this alloy, therefore ensuring more hardness and stability for the oxide layer, so decrease in the inflammatory responses in the soft tissues surrounding the implant will occur. Also, from Figure 7, it can be noticed that the metal ions released for M-TNZT alloy are lesser than these values for the TNZT sample. The presence of oxides and silver layer on the M-TNZT sample reduces the release of metal ions, this result indicates that the corrosion resistance of M-TNZT alloy is better than that of TNZT alloy, consistent with the results of the potentiodynamic polarization test. Also, Ag is not released from the M-TNZT sample due to the low amount of Ag in this alloy. It should be noted that silver already exists in the human body with a very low concentration of about 0.1–0.2 μg/L [34].

Antibacterial test result

Figure 8 shows the *S. aureus* and *E. coli* cultures after 24 hours for both samples using two

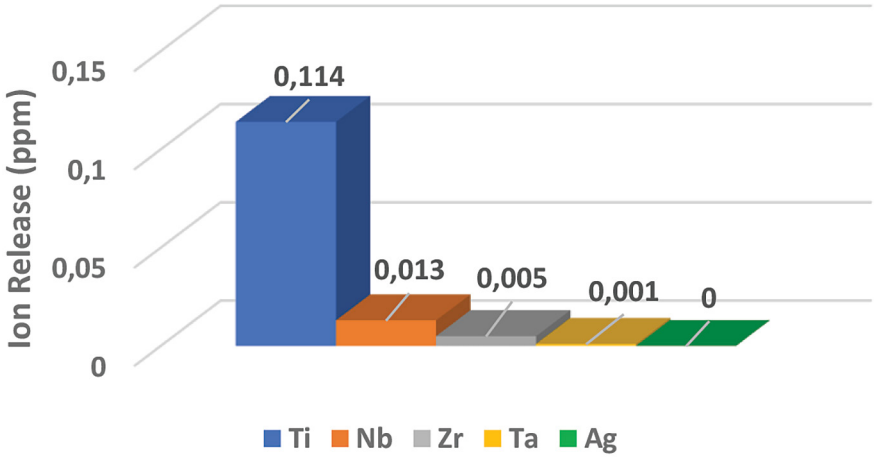

Figure 7. Quantity of metal ions released from M-TNZT alloy in SBF solution at 37 °C for 21 days

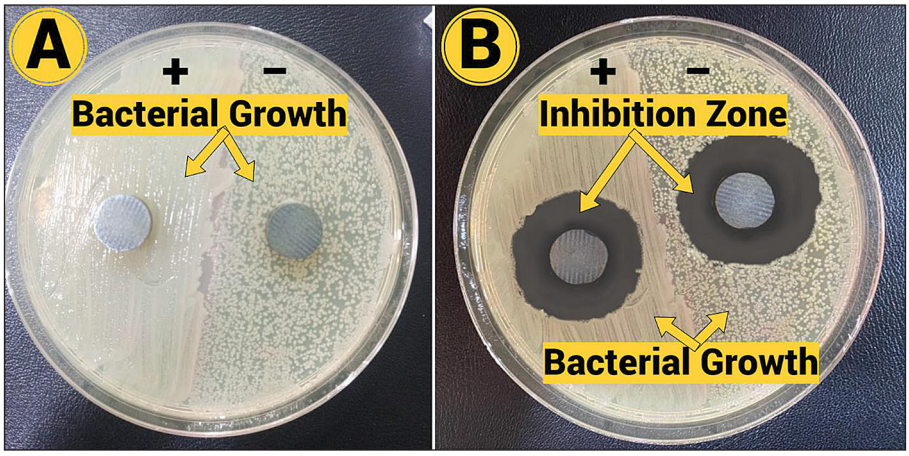

Figure 8. Images of the antibacterial tests using *S. aureus* and *E. coli* bacteria for (a) TNZT, and (b) M-TNZT sample

types of bacteria (*S. aureus*, Gr^+) and (*E. coli*, Gr^-). The formation of a clear region around the disc refers to the bacterial inhibition zone. It can be observed that the M-TNZT sample has a clear bacterial inhibition zone for both *S. aureus* and *E. coli* bacteria compared with the TNZT sample. This belongs to the strong antibacterial effect of Ag that is present on the surface of the M-TNZT sample. The four most prominent routes of antimicrobial action of Ag nanoparticles are [35]:

1. Ag particles adhere to the microbial cell surface and result in membrane damage and altered transport activity.
2. Ag particles penetrate inside the microbial cells and interact with cellular organelles and biomolecules, and thereby, affect respective cellular machinery.
3. Ag particles cause an increase in reactive oxygen species (ROS) inside the microbial cells leading to cell damage and
4. Ag particles modulate the cellular signal system, ultimately causing cell death.

On the other hand, since TNZT alloys lack antibacterial qualities and might become contaminated quickly after implantation, bacterial infection is a potential cause of failure, so enhancing the antibacterial property of this alloy is considered an extremely important issue [6].

The antibacterial characteristics of silver-containing surfaces were shown to be evident in the significant decrease of individual bacteria and bacterial clusters. The M-TNZT sample had the highest antibacterial effect compared with the TNZT sample. Due to its broad spectrum of antibacterial activity, silver is advantageous to both Gram-positive and Gram-negative bacteria [36]. Because of their interactions with the plasma membrane and the peptidoglycan cell wall membrane, as well as their interference with protein sulfhydryl groups, which prevents bacterial DNA replication, silver ions have antibacterial properties [37].

CONCLUSIONS

Surface modification for Ti-35Nb-7Zr-5Ta quaternary bio alloy fabricated by powder metallurgy was done using the PM-EDM route and valuable biocompatibility evaluation was done for this alloy before and after the modification treatment. The following results were obtained:

1. PM-EDM is an innovative method enabling simultaneous surface modification and implant shaping. The addition of powder improves the machining, mechanical, and biological properties of the PM-EDMed surface.
2. PM-EDM surface modification can extremely improve surface hardness, corrosion resistance, and biocompatibility as a whole.
3. Silver mixed-EDMed surface have higher hardness, corrosion resistance, and lower ion release due to the presence of Ag, oxides, and carbides such as NbC, TiC, TiO_2, ZrO_2, and Nb_2O_5 that are deposited and embedded as a hard phase in the recast layer of the machined surface.
4. Since TNZT alloys lack antibacterial qualities and might become contaminated quickly after implantation, bacterial infection is a potential cause of failure, so enhancing the antibacterial property of this alloy is considered an extremely important issue.

5. Due to its broad spectrum of antibacterial activity, silver is advantageous to both Gram-positive and Gram-negative bacteria. Because of their interactions with the plasma membrane and the peptidoglycan cell wall membrane, as well as their interference with protein sulfhydryl groups, which prevents bacterial DNA replication, silver ions have antibacterial properties. Thus, silver mixed-EDM effectively improved the antibacterial properties of this alloy.

Acknowledgements

The authors thank all the staff of the Material Engineering College, Metallurgical Engineering Department, University of Babylon-Iraq, for their persistent assistance during the experimentation processes of this research.

REFERENCES

1. Yadav P. and Saxena, K.K. Effect of heat-treatment on microstructure and mechanical properties of Ti alloys: An overview, in: Materials Today: Proceedings, 2019. doi: 10.1016/j.matpr.2020.02.541.
2. Niinomi M., Narushima T., and Nakai M., Advantages in metallic biomaterials, processing and applications. 2015.
3. Sowa M. et al., DC plasma electrolytic oxidation treatment of gum metal for dental implants, Electrochim Acta, 302, 2019, doi: 10.1016/j.electacta.2019.02.024.
4. Lee Y.S., M. Niinomi, M. Nakai, K. Narita, and K. Cho, Predominant factor determining wear properties of β-type and (α+β)-type titanium alloys in metal-to-metal contact for biomedical applications, J Mech Behav Biomed Mater, 41, 2015, doi: 10.1016/j.jmbbm.2014.10.005.
5. Yuan Z., He Y., Lin C., Liu P., and Cai K., Antibacterial surface design of biomedical titanium materials for orthopedic applications, Journal of Materials Science and Technology, 78, 2021. doi: 10.1016/j.jmst.2020.10.066.
6. Zhang Y., Chu K., He S., Wang B., Zhu W., and Ren F., Fabrication of high strength, antibacterial and biocompatible Ti-5Mo-5Ag alloy for medical and surgical implant applications, Materials Science and Engineering C, 106, 2020, doi: 10.1016/j.msec.2019.110165.
7. Vinodhini S.P. and Sridhar T.M., TiO_2 rutile phase formed interlayers by sintering monophasic bioceramics for biomedical applications, New Journal of Chemistry, 43(19), 2019, doi: 10.1039/c9nj01182j.
8. Furutani K., Sato H., and Suzuki M., Influence of electrical conditions on performance of electrical discharge machining with powder suspended in working oil for titanium carbide deposition process, International Journal of Advanced Manufacturing Technology, 40(11–12), 2009, doi: 10.1007/s00170-008-1420-x.
9. Furutania K., Saneto A., Takezawa H., Mohri N., and Miyake H., Accretion of titanium carbide by electrical discharge machining with powder suspended in working fluid, Precis Eng, 25(2), 138–144, 2001, doi: 10.1016/S0141-6359(00)00068-4.
10. Philip J.T., Mathew J., and Kuriachen B., Transition from EDM to PMEDM – Impact of suspended particulates in the dielectric on Ti6Al4V and other distinct material surfaces: A review, Journal of Manufacturing Processes, 64, 2021. doi: 10.1016/j.jmapro.2021.01.056.
11. Al-Amin M., Abdul Rani A.M., Abdu Aliyu A.A., Abdul Razak M.A., Hastuty S., and Bryant M.G., Powder mixed-EDM for potential biomedical applications: A critical review, Materials and Manufacturing Processes. 2020. doi: 10.1080/10426914.2020.1779939.
12. Meshramkar R., Shetty P., Nayak A., and Anehosur G. V., Surface treatment of zirconia implant, its surface roughness and its effect on osseointegration – a review, International Journal of Innovative Research in Medical Science, 4(5), 2019, doi: 10.23958/ijirms/vol04-i05/658.
13. Algodi S.J., Murray J.W., Fay M.W., Clare A.T., and Brown P.D., Electrical discharge coating of nanostructured TiC-Fe cermets on 304 stainless steel, Surf Coat Technol, 307, 2016, doi: 10.1016/j.surfcoat.2016.09.062.
14. Kruth J.-P., Stevens L., Froyen L., and Lauwers B., Study of the white layer of a surface machined by die-sinking electro-discharge machining, CIRP Annals, 44(1), 169–172, 1995, doi: 10.1016/S0007-8506(07)62299-9.
15. Furutania K., Saneto A., Takezawa H., Mohri N., and Miyake H., Accretion of titanium carbide by electrical discharge machining with powder suspended in working fluid, Precis Eng, 25(2), 138–144, 2001, doi: 10.1016/S0141-6359(00)00068-4.
16. Prakash C., Kansal H.K., Pabla B.S., and Puri S., Potential of powder mixed electric discharge machining to enhance the wear and tribological performance of <I>β</I>-Ti implant for orthopedic applications, Journal of Nanoengineering and Nanomanufacturing, 5(4), 2016, doi: 10.1166/jnan.2015.1245.
17. Prakash C. and Uddin M.S., Surface modification of β-phase Ti implant by hydroaxyapatite mixed electric discharge machining to enhance the corrosion resistance and in-vitro bioactivity, Surf Coat Technol, vol. 326, 2017, doi: 10.1016/j.surfcoat.2017.07.040.
18. Davis R. et al., Enhanced micro-electric discharge machining-induced surface modification on biomedical Ti-6Al-4V alloy, J Manuf Sci Eng, 144(7),

2022, doi: 10.1115/1.4053110.

19. Schubert A., Bui V.D., Schaarschmidt I., Berger T., and Martin A., Developments in powder mixed EDM and its perspective application for targeted surface modification, Procedia CIRP, 113, 100–119, 2022, doi: 10.1016/j.procir.2022.09.134.
20. Nauryz N., Omarov S., Kenessova A., Pham T.T., Talamona D., and Perveen A., Powder-mixed micro-electro-discharge machining-induced surface modification of titanium alloy for antibacterial properties, Journal of Manufacturing and Materials Processing, 7(6), 214, 2023, doi: 10.3390/jmmp7060214.
21. ASTM E10-15, Standard test method for brinell hardness of metallic materials, ASTM International, no. June, 2012.
22. ASTM G5-14, ASTM G5 Standard reference test method for making potentiodynamic anodic polarization measurements, Annual Book of ASTM Standards, 2014.
23. Rao S.B. and Chowdhary R., Evaluation on the corrosion of the three Ni-Cr alloys with different composition, Int J Dent, 2011, doi: 10.1155/2011/397029.
24. JSA-JIS T 0304, Testing method for metal release from metallic biomaterials, JSA, Jul. 2022.
25. Bhargav H.S., Shastri S.D., Poornav S.P., Darshan K.M., and Nayak M.M., Measurement of the zone of inhibition of an antibiotic, in: Proceedings of 6th International Advanced Computing Conference, IACC 2016, 2016. doi: 10.1109/IACC.2016.82.
26. ISO 20645, Textile fabrics. Determination of antibacterial activity: Agar diffusion plate test, International Organization for Standardization, ISO. 2004.
27. Meerson G.A. and Segorcheanu T., The affinity of niobium for oxygen, Soviet Atomic Energy, 13(6). 1963. doi: 10.1007/BF01312333.
28. Weeks J.R., Neutron absorber materials for reactor control. Nuclear Science and Engineering, 15(1), 1963, doi: 10.13182/nse63-a26270.
29. Prakash C., Kansal H.K., Pabla B.S., and Puri S., Processing and characterization of novel biomimetic nanoporous bioceramic surface on β-Ti implant by powder mixed electric discharge machining, J Mater Eng Perform, 24(9), 2015, doi: 10.1007/s11665-015-1619-6.
30. Chang-Bin T., Dao-Xin L., Zhan W., and Yang G., Electro-spark alloying using graphite electrode on titanium alloy surface for biomedical applications, Appl Surf Sci, 257(15), 2011, doi: 10.1016/j.apsusc.2011.01.120.
31. Scully J.R., Budiansky N.D., Tiwary Y., Mikhailov A.S., and Hudson J.L., An alternate explanation for the abrupt current increase at the pitting potential, Corrosion Science, 50(2), 2008. doi: 10.1016/j.corsci.2007.08.002.
32. Zhang Y., Davenport A.J., Burke B., Vyas N., and Addison O., Effect of Zr addition on the corrosion of Ti in acidic and reactive oxygen species (ROS)-containing environments, ACS Biomater Sci Eng, 4(3), 2018, doi: 10.1021/acsbiomaterials.7b00882.
33. Azharuddin M. et al., A repertoire of biomedical applications of noble metal nanoparticles, Chemical Communications, 55(49), 2019, doi: 10.1039/c9cc01741k.
34. Armitage S.A., White M.A., and Wilson H.K., The determination of silver in whole blood and its application to biological monitoring of occupationally exposed groups, Annals of Occupational Hygiene, 40(3), 1996, doi: 10.1016/0003-4878(95)00076-3.
35. Dakal T.C., Kumar A., Majumdar R.S., and Yadav V., Mechanistic basis of antimicrobial actions of silver nanoparticles, Front Microbiol, 7, 2016, doi: 10.3389/fmicb.2016.01831.
36. Suresh A.K. et al., Silver nanocrystallites: Biofabrication using shewanella oneidensis, and an evaluation of their comparative toxicity on gram-negative and gram-positive bacteria, Environ Sci Technol, 44(13), 2010, doi: 10.1021/es903684r.
37. Patil M.P. and Do Kim G., Eco-friendly approach for nanoparticles synthesis and mechanism behind antibacterial activity of silver and anticancer activity of gold nanoparticles, Applied Microbiology and Biotechnology, 101(1), 2017. doi: 10.1007/s00253-016-8012-8.